Electronic Supplementary Material (ESI) for Journal of Materials Chemistry A.


**Supplementary Information**

# One-step Construction of Core/Shell Nanoarrays with Holey Shell and Exposed Interfaces for Overall Water Splitting

Qingliang Lv, [a] Lei Yang,[a] Wei Wang,[a, b] **Siqi Lu, [a] Tianen Wang, [a]** Lixin Cao,*[a] and Bohua Dong*[a]

[a] School of Materials Science and Engineering, Ocean University of China, 238 Songling Road, Qingdao, 266100 P. R. China.

[b] Aramco Research Center Boston, Aramco Services Company, Cambridge, MA02139, USA.

*Corresponding authors' Emails: dongbohua@ouc.edu.cn (B. Dong) and caolixin@ouc.edu.cn (L. Cao)

The possible reactions in the one-step synthesis of $Ni_3S_2/VO_2$ core/shell nanoarrys:

$$CH_3CSNH_2 + H_2O \longrightarrow CH_3CONH_2 + H_2S\uparrow$$

$$3Ni + 2H_2S \longrightarrow Ni_3S_2 + 2H_2\uparrow$$

$$Na_3VO_4 + 4H_2O \xrightarrow{\Delta} NaVO_3 + 2NaOH$$

$$2NaVO_3 + 4H_2 \longrightarrow V_2O_3 + 2NaOH$$

$$2V_2O_3 + O_2 \longrightarrow 4VO_2$$

**Table S1** OER comparison of the electrocatalytic performance of $Ni_3S_2/VO_2$ with some representative bifunctional electrocatalysts reported recently

| Electrocatalyst | Electrolyte | η [mV] for $j_{OER}$ =10 mA $cm^{-2}$ | Tafel slope [mV $dec^{-1}$] | Reference |
|---|---|---|---|---|
| $Ni_3S_2/VO_2$ | 1M KOH | 150 | 47 | This work |
| $Co(S_xSe_{1-x})_2$ | 1M KOH | 283 | 65.6 | Adv. Funct. Mater. 2017, 27, 1701008 |
| $Co_3O_4$-MTA | 1M KOH | 290 | 84 | Angew. Chem. Int. Ed. 2017, 56, 1324-1328 |
| NiFe LDH-NS@DG | 1M KOH | 210 | 52 | Adv. Mater. 2017, 29, 1700017 |
| δ-FeOOH NSs/NF | 1M KOH | 265 | 36 | Adv. Mater. 2018, 1803144 |
| $Co_9S_8$@NOSC-900 | 1M KOH | 340 | 68 | Adv. Funct. Mater. 2017, 27, 1606585 |
| Cu@CoSx/CF | 1M KOH | 160 | - | Adv. Mater. 2017, 29, 1606200 |
| NCP | 1M KOH | 280 | - | J. Am. Chem. Soc. 2018, 140, 5241-5247 |
| $Ni_xCo_{3-x}S_4/Ni_3S_2/NF$ | 1M KOH | 160 | 95 | Nano Energy 35 (2017) 161-170 |
| $Fe_{0.09}Co_{0.13}$-$NiSe_2$/CFC | 1M KOH | 251 | 89 | Adv. Mater. 2018, 1802121 |
| 2.5H-PHNCMs | 1M KOH | 235 | 45.7 | Nat Commun 2017, 8, 15377 |
| IFONFs-45 | 1M KOH | 260 | 45 | Nat Commun 2018, 9, 1809 |
| FeCoNi-HNTAs | 1M KOH | 184 | 49.9 | Nat Commun 2018, 9, 2452 |
| Am $FePO_4$ | 1M KOH | 218 | 42.72 | Adv. Mater. 2017, 1704574 |
| FeP/$Ni_2P$ | 1M KOH | 154 | 22.7 | Nat Commun 2018, 9, 2551 |
| PNGF (op) | 1M KOH | 320 | 86 | Energy Environ. Sci. 2017, 10, 1186 |
| A-$CoS_{4.6}O_{0.6}$ PNCs | 1M KOH | 290 | 69 | Angew. Chem. Int. Ed. 2017, 56, 4858 |
| P-CC | 1M KOH | 450 | 65 | Adv. Mater. 2017, 29, 1606027 |
| CoNi(20 : 1)-P-NS | 1M KOH | 273 | 52 | Energy Environ. Sci. 2017,10, 893 |
| pc-Ni-$B_i$@NB | 1M KOH | 302 | 52 | Angew. Chem. Int. Ed. 2017, 56, 6572 |
| $Au_{0.89}Fe_{0.11}$ NPs | 1M KOH | 800 | - | Angew. Chem. Int. Ed. 2017, 56, 6589 |
| NCNTFs | 1M KOH | 370 | 64 | Nature Energy 2016, 1, 15006 |
| VOOH nanospheres | 1M KOH | 227 | 68 | Angew. Chem. Int. Ed. 2017, 56, 573 |
| NC/CuCo/CuCoOx | 1M KOH | 198 | 88 | Adv. Funct. Mater. 2018, 28, 1704447 |
| Se-(NiCo)S/OH | 1M KOH | 155 | 34 | Adv. Mater. 2018, 30, 1705538 |
| $MoS_2/Ni_3S_2$ | 1M KOH | 218 | 88 | Angew. Chem. Int. Ed. 2016, 55, 6702-6707 |
| $Co_3S_4$@$MoS_2$ | 1M KOH | 280 | 43 | Nano Energy 47 (2018) 494-502 |

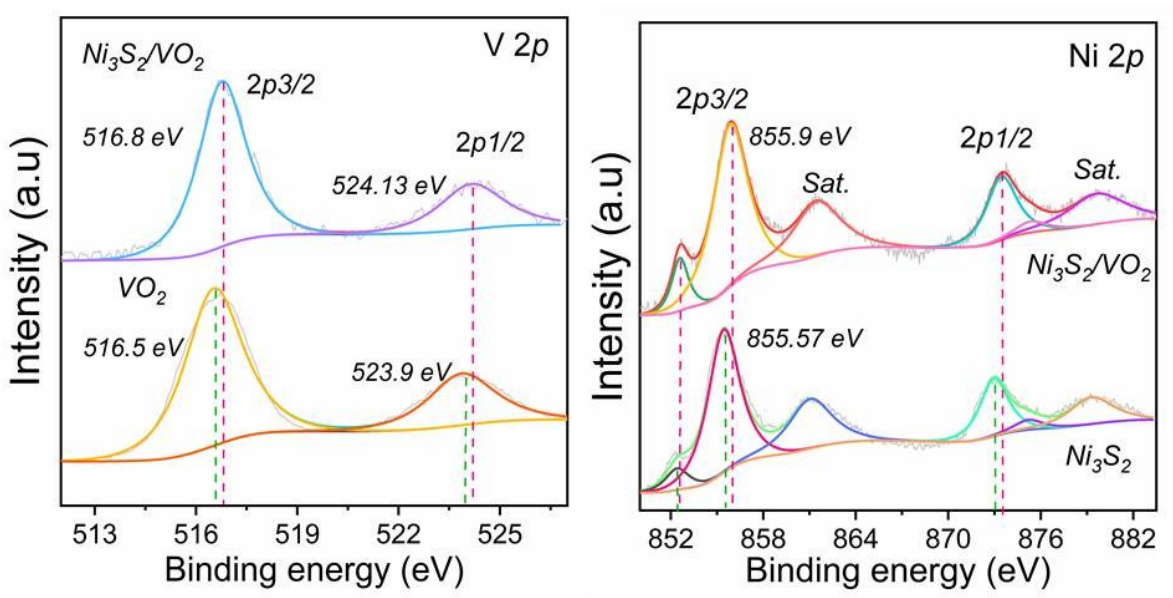


**Figure S1.** The changes of V 2p and Ni 2p of $Ni_3S_2/VO_2$ before and after the heterogenous structures formed.

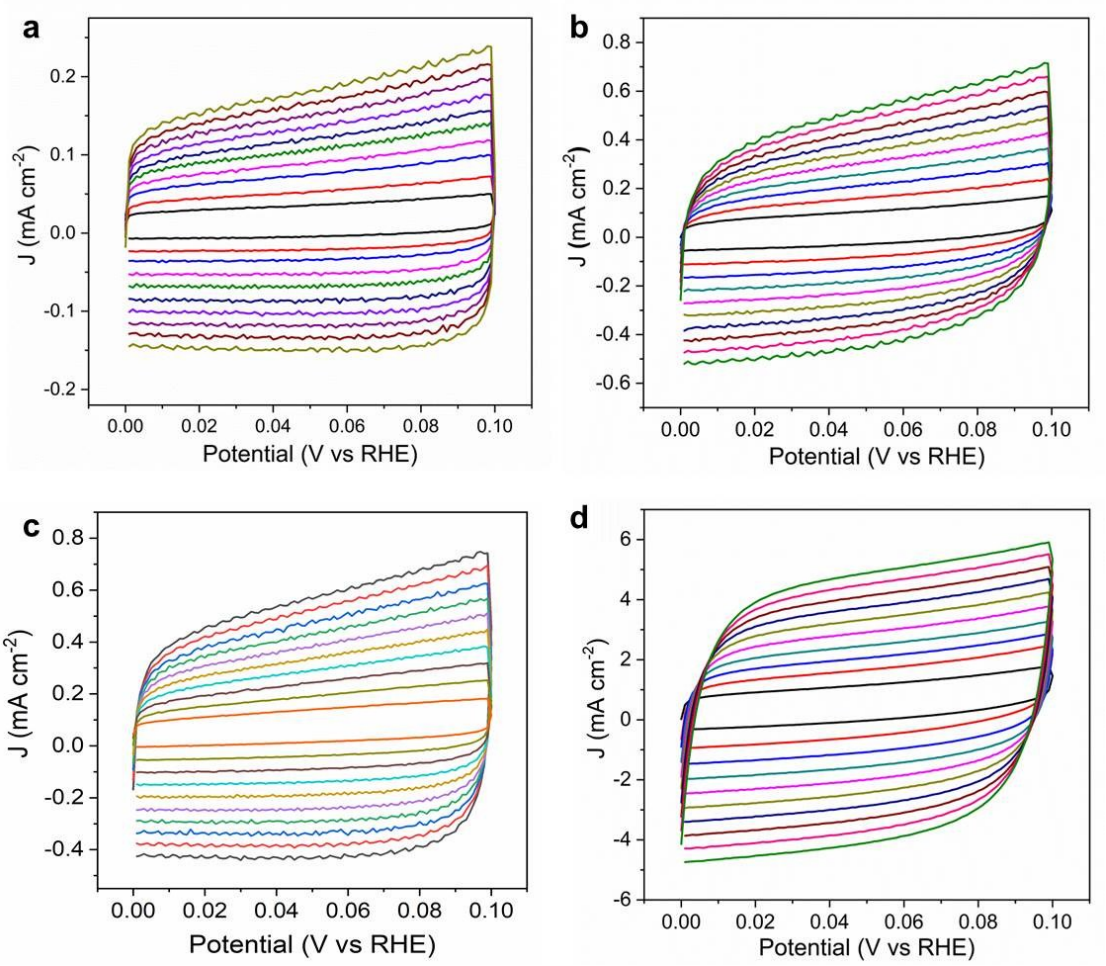


**Figure S2.** The electrochemically active surface area (EASA) was estimated from the electrochemical double-layer capacitance. The electrochemical capacitance was determined from cyclic voltammograms measured in a non-Faradaic region at different scan rates. The ECSA was measured to evaluate the exposed catalytically active sites in the materials. (a) Ni foam; (b) $Ni_3S_2$; (c) $VO_2$ ; (d) $Ni_3S_2/VO_2$

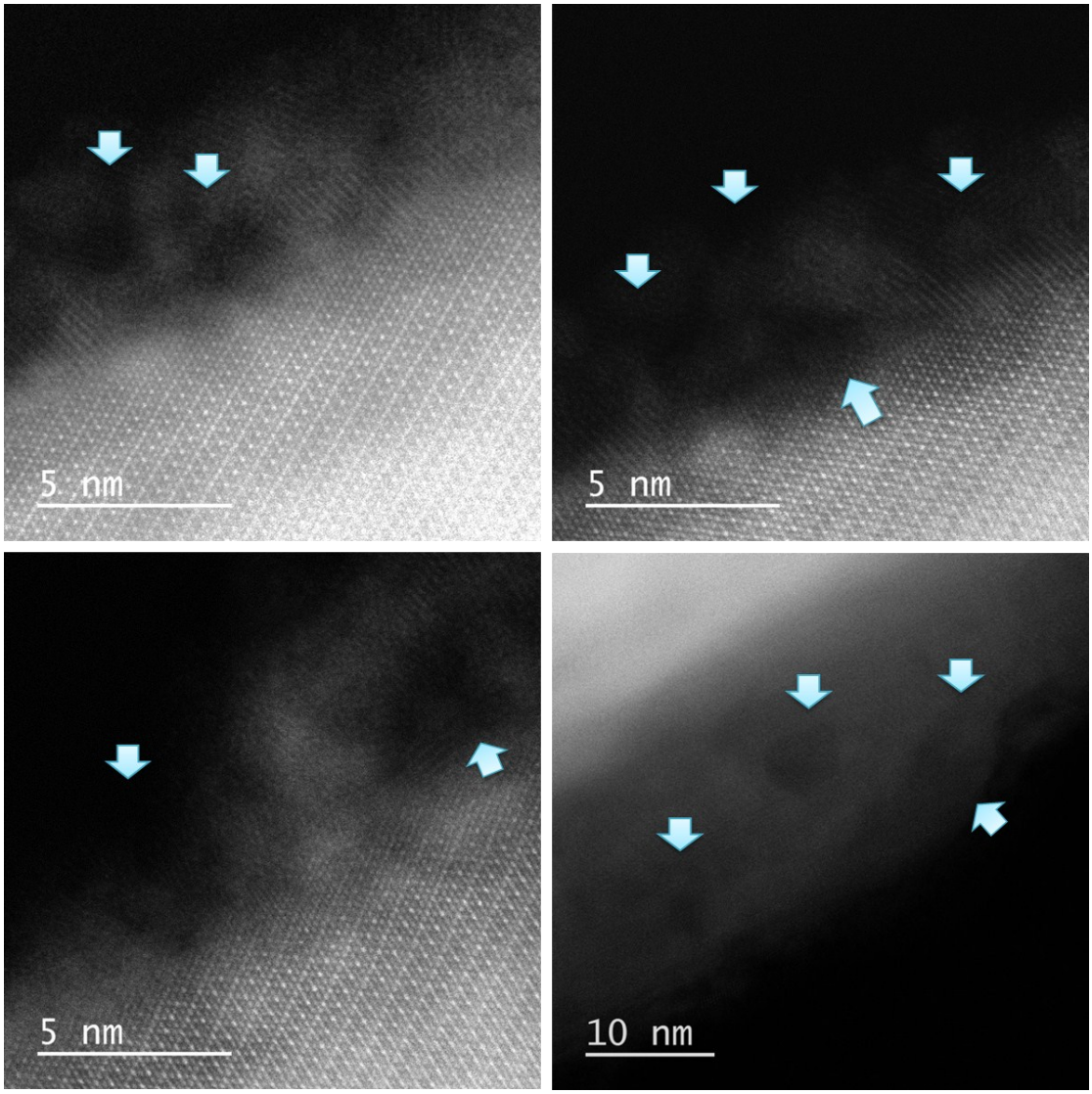


**Figure S3.** Typical HAADF-STEM images of a single $Ni_3S_2/VO_2$ nanowire with numerous pores and exposed interfaces.

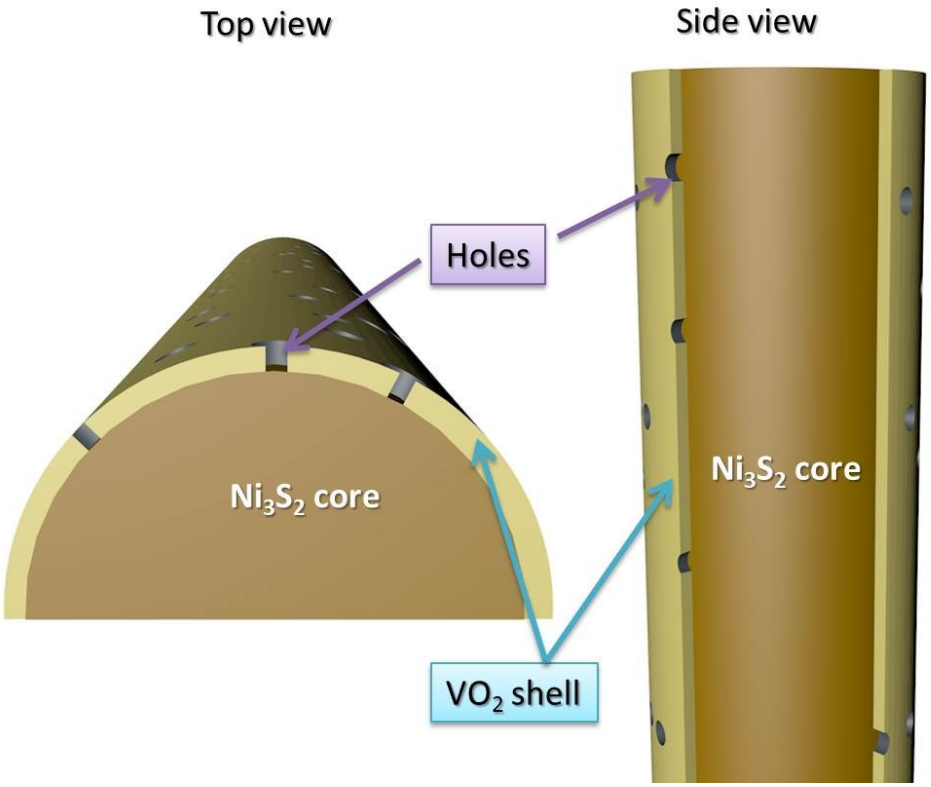


**Figure S4.** Illustration of holes formed on $VO_2$ the shell

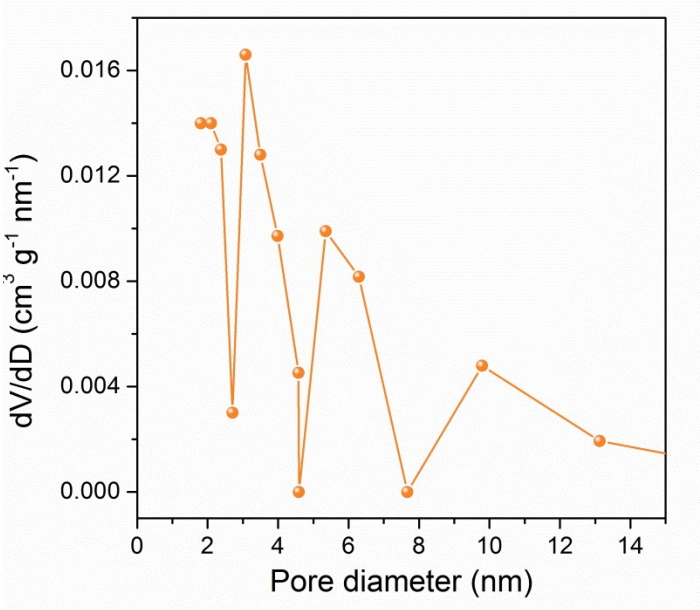


**Figure S5.** The pore size distribution of $Ni_3S_2/VO_2$

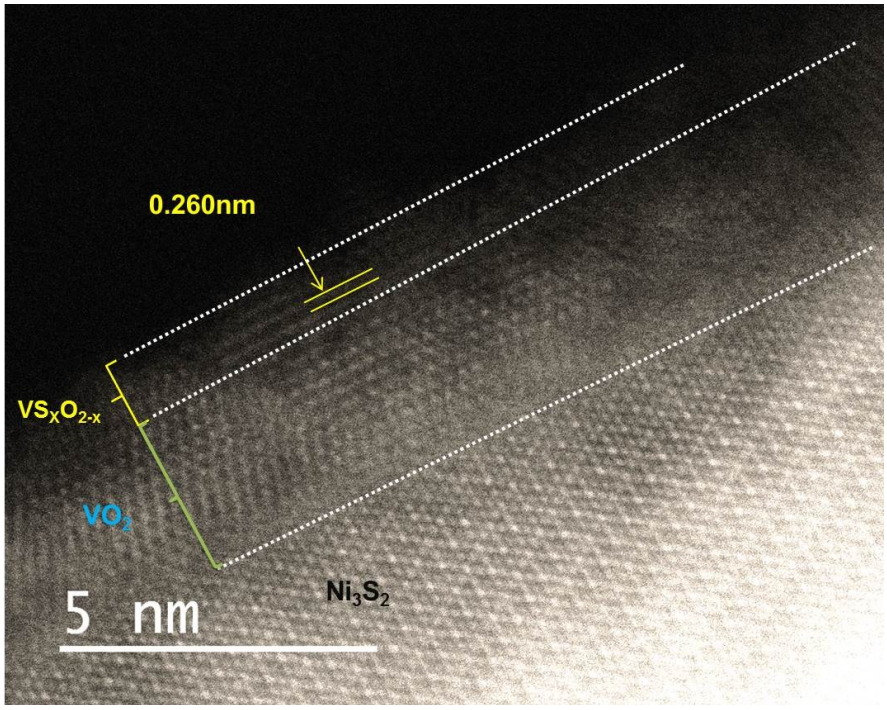


**Figure S6.** Typical HAADF-STEM images of $VS_xO_{2-x}$ layer on the surface of $Ni_3S_2/VO_2$

*Method and Model:* The models of $Ni_3S_2$ and $VO_2$ have been built, the surfaces of them have been cut along the (1 -2 1) and (-2 1 1) directions, respectivily, and the vacuum space along the z direction is set to be 15 Å, which is enough to avoid interaction between the two neighboring images. Six different interfaces between $Ni_3S_2$ and $VO_2$ have been built considering about the relative locations and the most stable interface has been used in the next. Then, O*, OH* and OOH* groups have been absorbed on the substrate surfaces and interfaces. The first principles calculations in the framework of density functional theory, including structural, electronic performances, were carried out based on the Cambridge Sequential Total Energy Package known as CASTEP. The exchange–correlation functional under the generalized gradient approximation (GGA) with norm-conserving pseudopotentials and Perdew–Burke–Ernzerhof functional was adopted to describe the electron–electron interaction.[3] An energy cutoff of 750 eV was used and a k-point sampling set of 5 x 5 x 1 were tested to be converged. A force tolerance of 0.01 eV $Å^{-1}$, energy tolerance of $5.0x10^{-7}$eV per atom and maximum displacement of $5.0x10^{-4}$ Å were considered. Each atom in the storage models is allowed to relax to the minimum in the enthalpy without any constraints. Adsorption energy $E_{ads}$ of A (=O, OH and OOH) group on the surface of substrates was defined as:

$E_{ads}=E_{*A}–(E_{*}+E_A)$

where *A and * denote the adsorption of A on substrates and the bare substrates, $E_A$ denotes the energy of A group.

Free energy change ΔG of the reaction was calculated as the difference between the free energies of the initial and final states as shown below:

$\Delta G=\Delta E + \Delta ZPE – T\Delta S + \Delta G_U + \Delta G_{pH}$

where E is the calculated energy by DFT, ZPE is the zero point energy, S denotes the entropy, $\Delta G_U=-eU$ (e is the elementary positive charge, U is the potential of the photogenerated carrier vs normal hydrogen electrode) and $\Delta G_{pH}$ $=-2.303k_BT$ pH. Here, $k_B$ is the Boltzmann constant, T= 300K and pH =0 have been considered. The vibrational frequencies were calculated through DFT to obtain the ZPE and S values. The free energy of $H^+/ e^-$ pair is considered as half of free energy of $H_2$. The free

energy of $O_2$ has been calculated from the free energy change (4.92 eV) of the reaction $2H_2 + O_2 \rightarrow 2H_2O$.

$* + H_2O \rightarrow OH* + (H^+ + e^-)$ (1)

$OH* \rightarrow O* + (H^+ + e-)$ (2)

$O* + H_2O \rightarrow OOH* + (H^+ + e^-)$ (3)

$OOH* \rightarrow * + O_2 + (H^+ + e^-)$ (4)

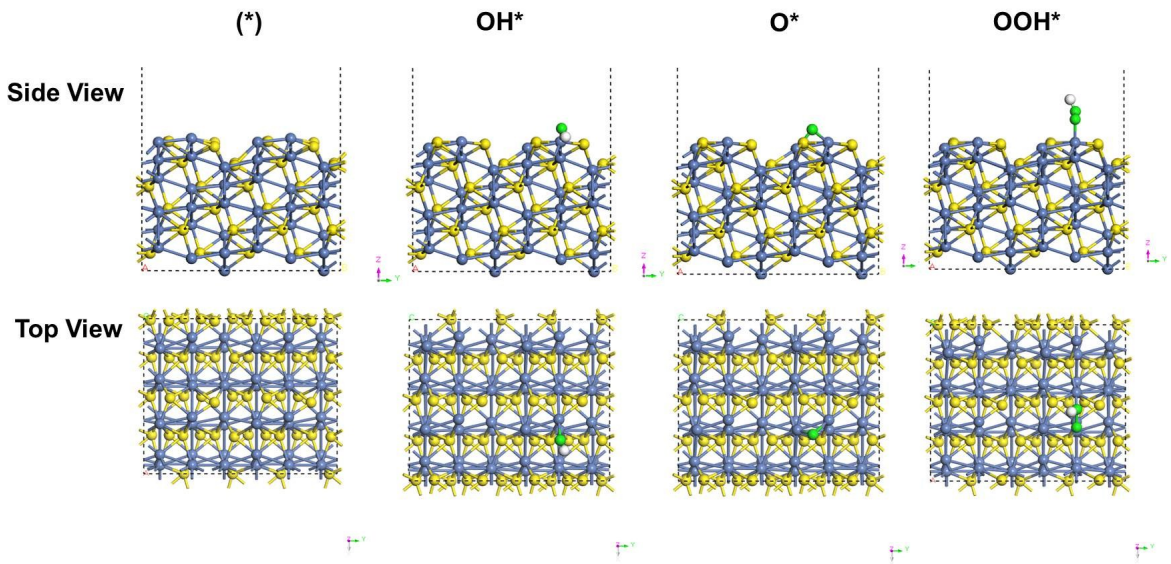


**Figure S7.** Optimized structures of the intermediate states in OER on surface of $Ni_3S_2$ (1 -2 1)

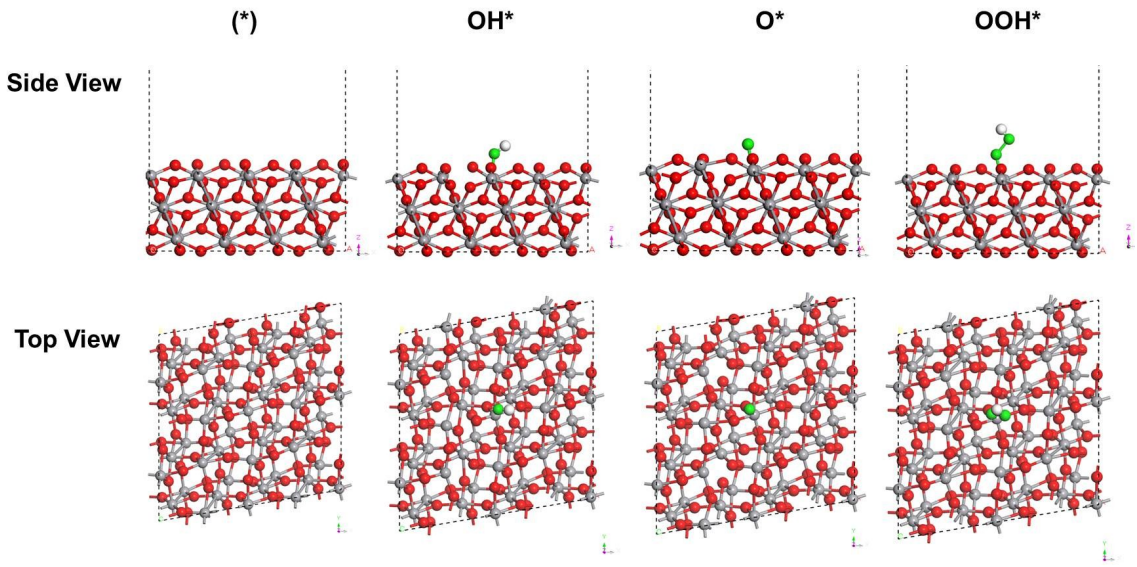


**Figure S8.** Optimized structures of the intermediate states in OER on surface of $VO_2$ (-2 1 1)

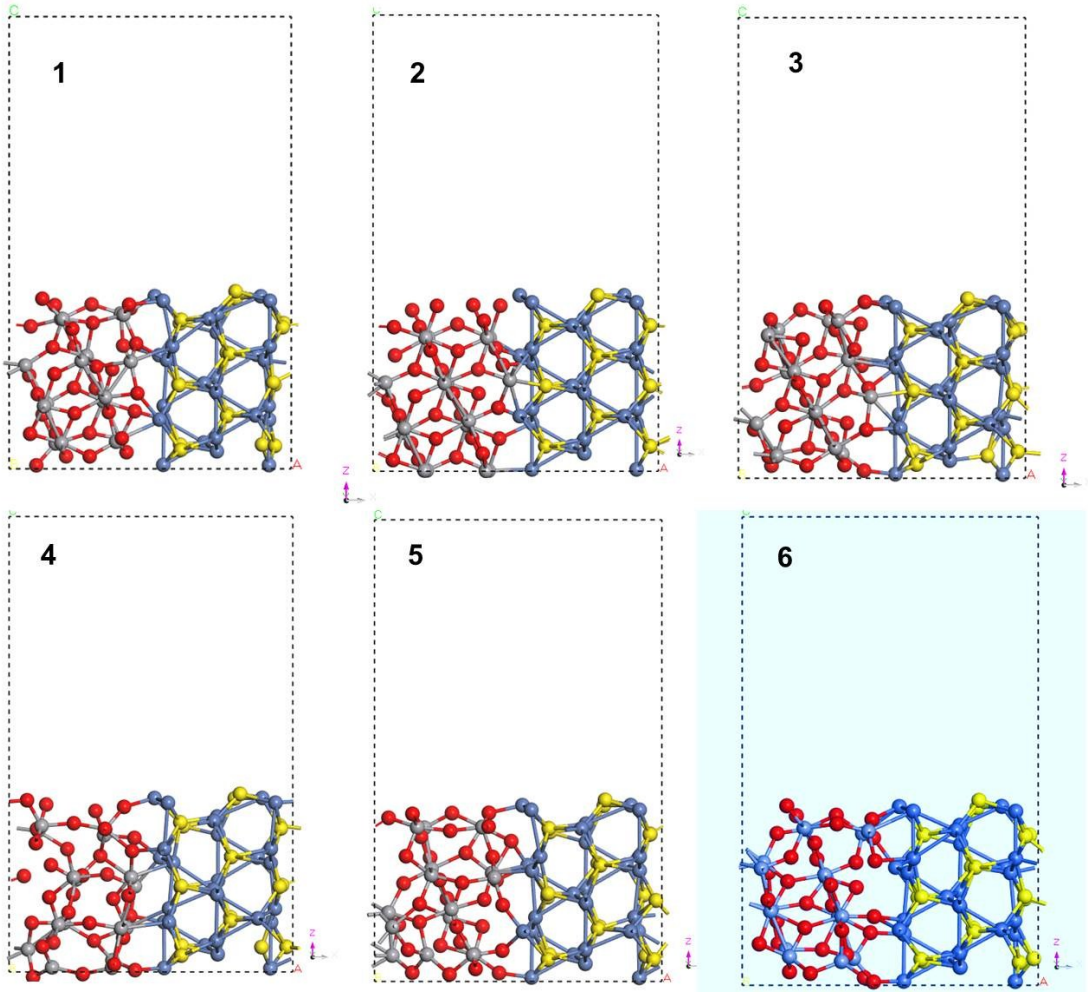


**Figure S9.** Six different interfaces between $Ni_3S_2$ and $VO_2$ . The most stable interface in 6 has been used.

**Table S2.** The corresponding energy in Figure S6.

| Interfaces | Total energy (eV) |
|---|---|
| 1 | -87037.1769 |
| 2 | -87032.3258 |
| 3 | -87037.7090 |
| 4 | -87033.1159 |
| 5 | -87037.6800 |
| 6 | -87039.9248 |

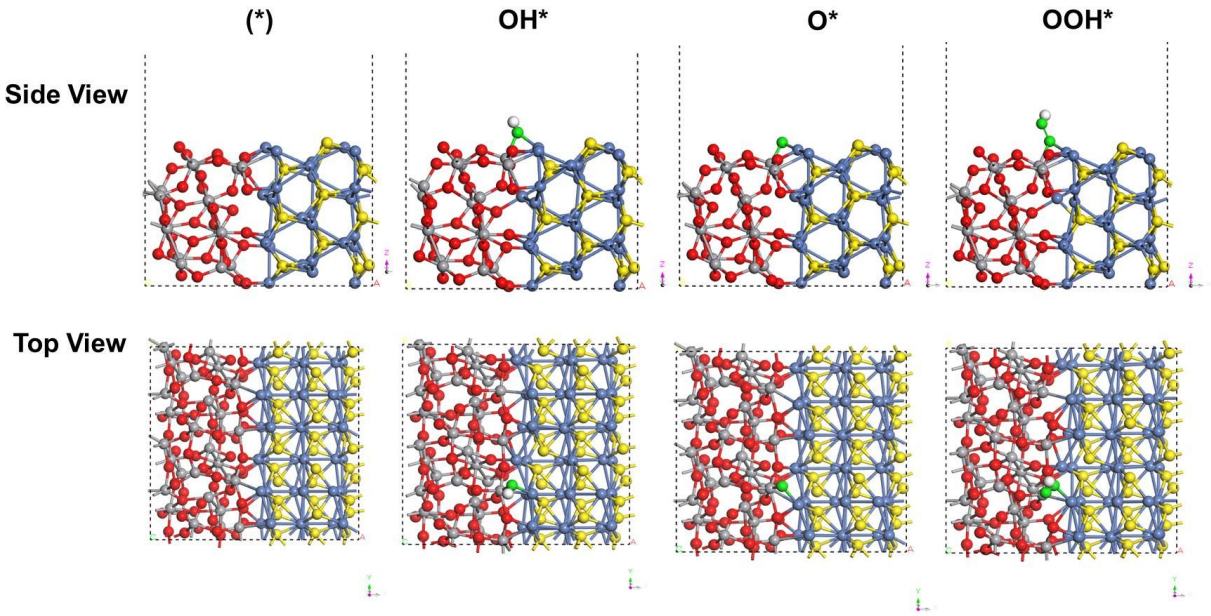


**Figure S10.** Optimized interfaces of the intermediate states in OER on interface of $Ni_3S_2/VO_2$

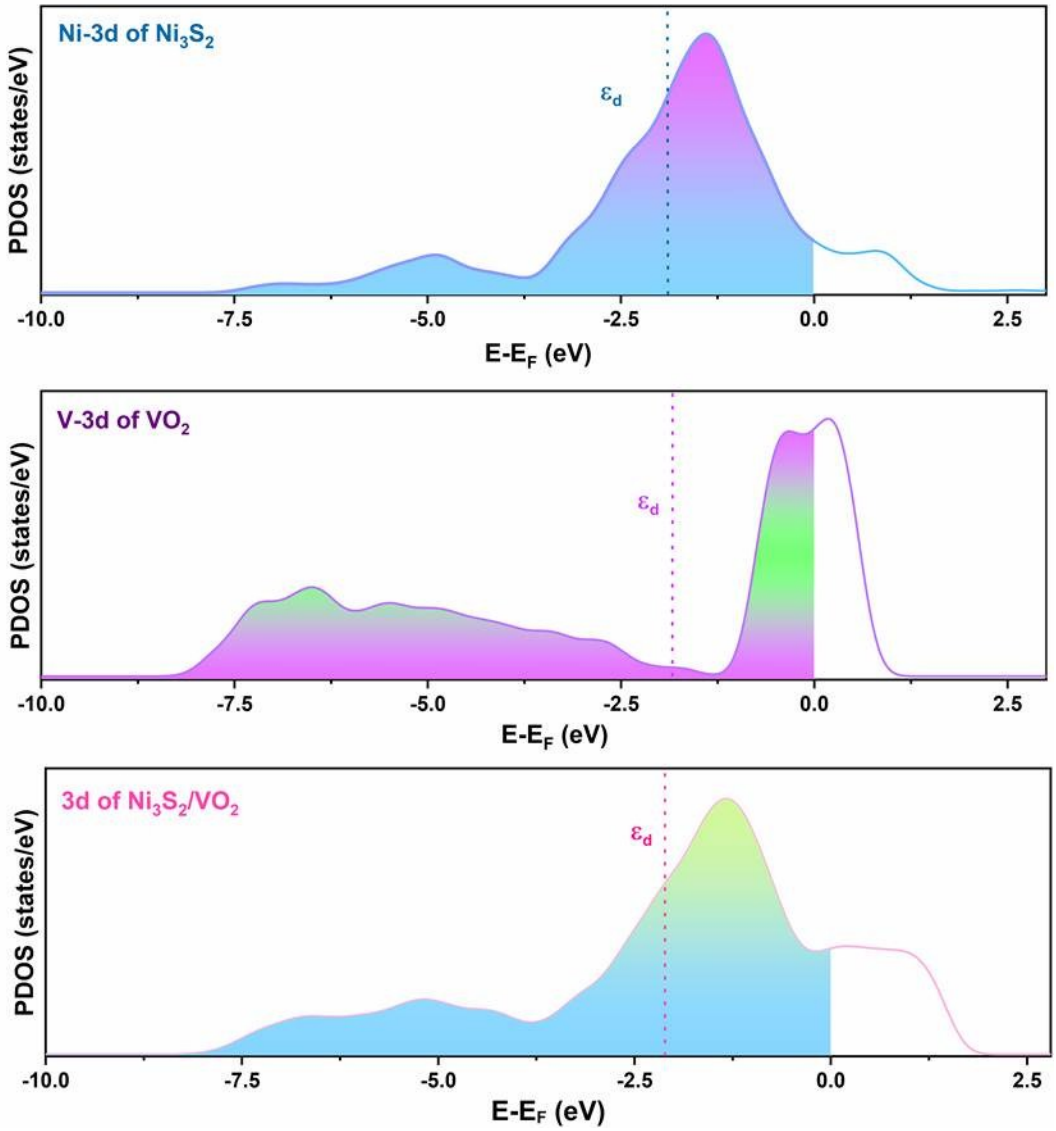


**Figure S11.** Calculated PDOS of the d band of the Ni, V atoms in $Ni_3S_2$, $VO_2$ and $Ni_3S_2/VO_2$ The d band center is marked by the pink dashed line, and the Fermi level is set as zero.

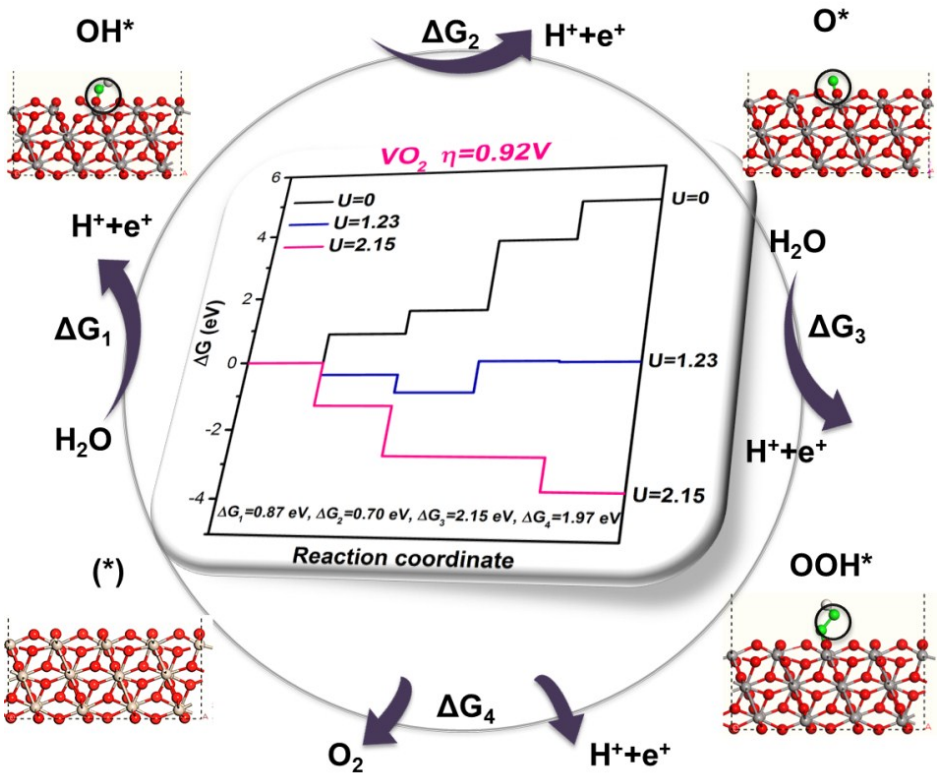


**Figure S12.** Schematic of the OER process on the surface of $VO_2$ (-2 1 1).

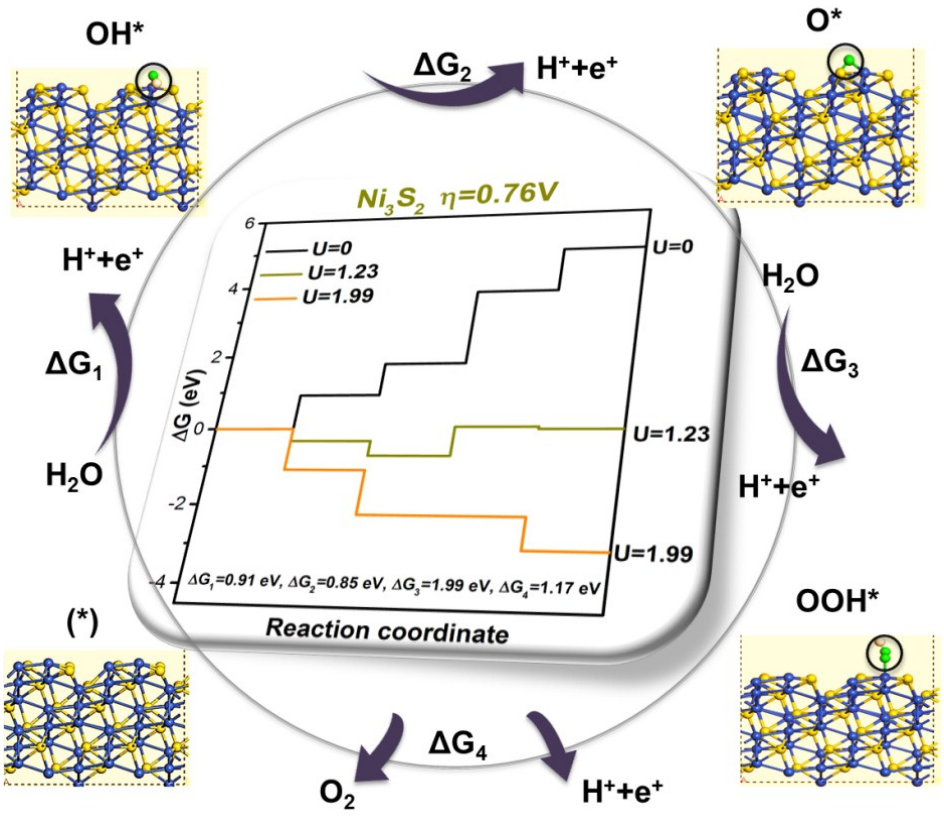


**Figure S13.** Schematic of the OER process on the surface of $Ni_3S_2$ (1 -2 1)

**Table S3** Comparison of the electrocatalytic performance of $Ni_3S_2/VO_2$ with some representative bifunctional electrocatalysts reported recently for overall water splitting

| Electrocatalyst | Electrolyte | η [V] for $j_{OWS}$ = 10 mA $cm^{-2}$ | η [V] for $j_{OWS}$ = 20 mA $cm^{-2}$ | η [V] for $j_{OWS}$ = 100 mA $cm^{-2}$ | Reference |
|---|---|---|---|---|---|
| $Ni_3S_2/VO_2$ | 1M KOH | 1.42 | 1.45 | 1.65 | This work |
| $MoS_2/Ni_3S_2$ | 1M KOH | 1.56 | 1.62 | 1.7 | Angew. Chem. Int. Ed. 2016, 55, 6702 |
| VOOH nanospheres | 1M KOH | 1.62 | 1.7 | 1.85 | Angew. Chem. Int. Ed. 2017, 56, 573 |
| Ni@NC-800/Ni foam | 1M KOH | 1.60 | 1.66 | 1.98 | Adv. Mater. 2017, 29, 1605957 |
| $Co_3S_4@MoS_2$ | 1M KOH | 1.58 | 1.62 | 1.85 | Nano Energy. 2018,47 494-502 |
| NiFe-MOF array | 1M KOH | 1.55 | 1.6 | 1.71 | Nature Commun. 2017, 8, 15341 |
| NC/CuCo/CuCoOx | 1M KOH | 1.53 | 1.57 | 1.75 | Adv. Funct. Mater. 2018, 28, 1704447 |
| Se-(NiCo)S/OH | 1M KOH | 1.6 | 1.65 | 2.05 | Adv. Mater. 2018, 30, 1705538 |
| FeCoNi-HNTAs | 1M KOH | 1.429 | 1.49 | 1.706 | Nat Commun 2018, 9, 2452 |
| 2.5H-PHNCMs | 1M KOH | 1.44 | 1.50 | - | Nat Commun 2017, 8, 15377 |
| IFONFs-45 | 1M KOH | 1.58 | 1.62 | - | Nat Commun 2018, 9, 1809 |
| Am $FePO_4$ | 1M KOH | 1.54 | 1.58 | 1.72 | Adv. Mater. 2017, 1704574 |
| $FeP/Ni_2P$ | 1M KOH | 1.42 | 1.48 | 1.62 | Nat Commun 2018, 9, 2551 |
| Ni@NC-800/Ni foam | 1M KOH | 1.60 | 1.66 | 1.98 | Adv. Mater. 2017, 29, 1605957 |
| A-PBCCF-H NFs | 1M KOH | 1.56 | 1.65 | 1.8 | Nano Energy 2017, 32 247 |
| NiFe-MOF array | 1M KOH | 1.55 | 1.6 | 1.71 | Nature Commun. 2017, 8, 15341 |
| EG/H-$Co_{0.85}Se$\|P | 1M KOH | 1.64 | 1.85 | - | Adv. Mater. 2017, 29, 1701589 |
| $Co(S_xSe_{1-x})_2$ | 1M KOH | 1.63 | 1.7 | 1.95 | Adv. Funct. Mater. 2017, 27, 1701008 |
| $Co_3O_4$-MTA | 1M KOH | 1.61 | 1.7 | 2 | Angew. Chem. Int. Ed. 2017, 56, 1324-1328 |
| NiFe LDH-NS@DG | 1M KOH | 1.45 | 1.5 | 1.8 | Adv. Mater. 2017, 29, 1700017 |
| δ-FeOOH NSs/NF | 1M KOH | 1.63 | - | - | Adv. Mater. 2018, 1803144 |
| $Co_9S_8$@NOSC-900 | 1M KOH | 1.6 | 1.74 | 2 | Adv. Funct. Mater. 2017, 27, 1606585 |
| Cu@CoSx/CF | 1M KOH | 1.5 | 1.59 | 1.8 | Adv. Mater. 2017, 29, 1606200 |
| NCP | 1M KOH | 1.56 | 1.69 | 1.92 | J. Am. Chem. Soc. 2018, 140, 5241-5247 |
| $Ni_xCo_{3-x}S_4/Ni_3S_2/NF$ | 1M KOH | 1.53 | 1.62 | 1.80 | Nano Energy 35 (2017) 161-170 |
| $Fe_{0.09}Co_{0.13}$-$NiSe_2$/CFC | 1M KOH | 1.52 | 1.57 | 1.67 | Adv. Mater. 2018, 1802121 |
| NiO NRs | 1M KOH | 1.62 | 1.66 | - | Nano Energy 43 (2018) 103-109 |

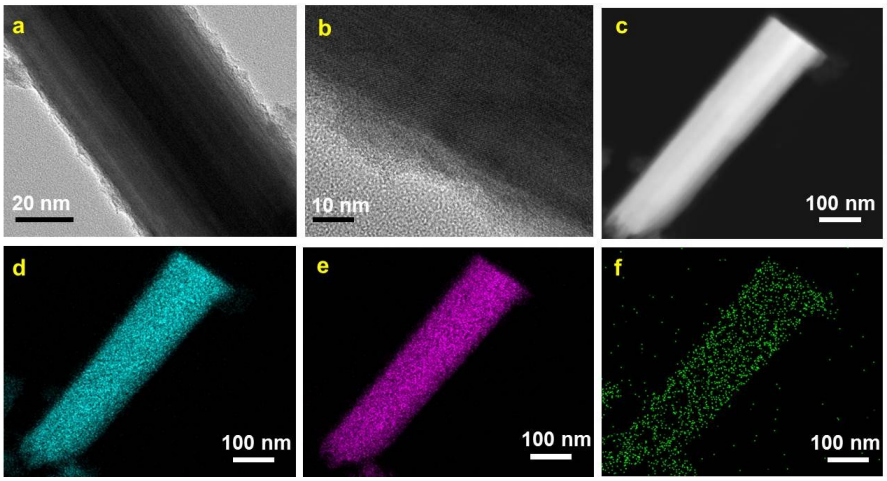


**Figure S14.** TEM image, HAADF-STEM image of and element mapping images of Ni (d), S (e), and V (f) of $Ni_3S_2/VO_2$ CSN after water splitting test

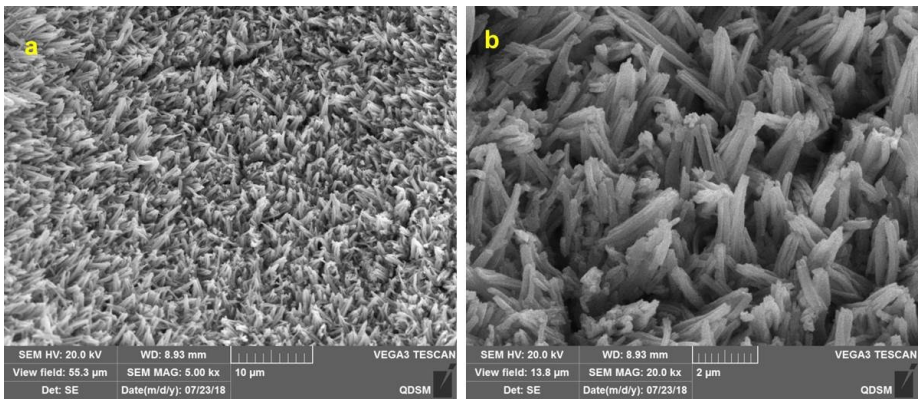


**Figure S15.** SEM image of $Ni_3S_2/VO_2$ **CSN** after water splitting test.

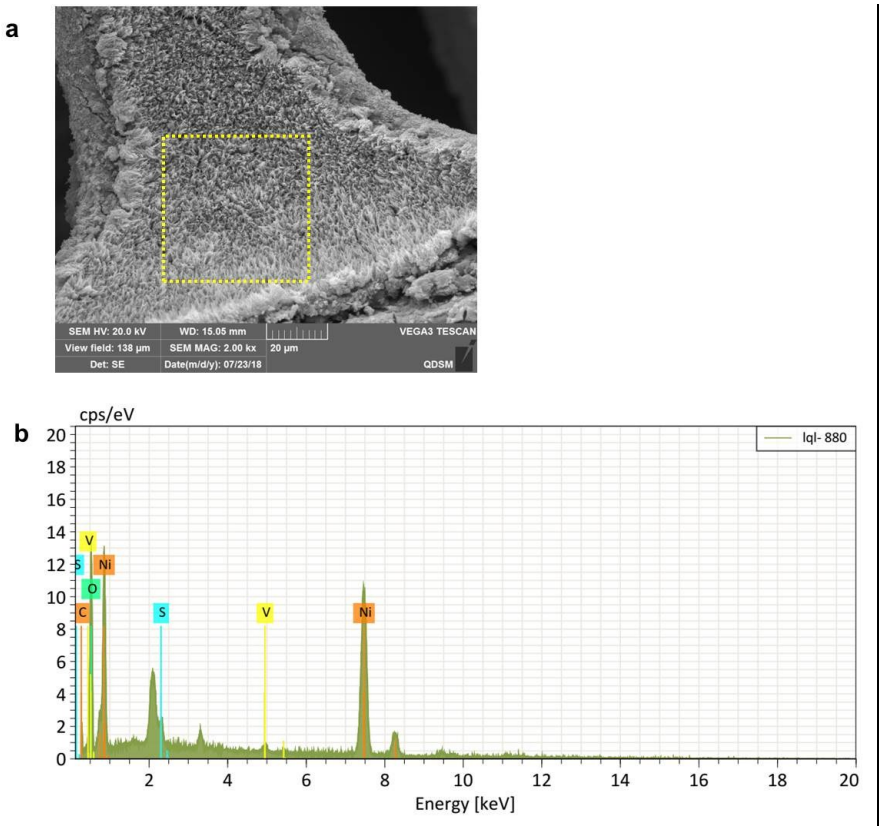


**Figure S16.** The EDS spectrum of the elements V, Ni, S and O of $Ni_3S_2/VO_2$ CSN after water splitting test.

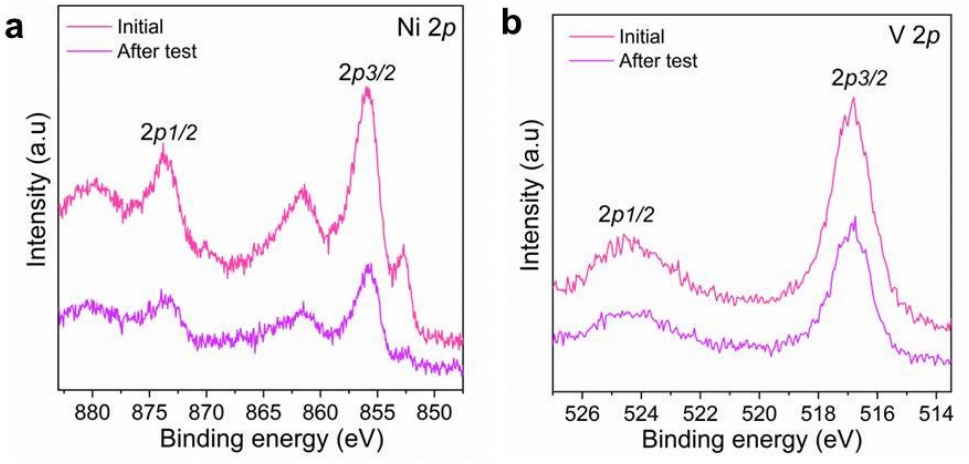


**Figure S17.** XPS spectra of Ni 2p and V 2p binding energies before and after water splitting test.

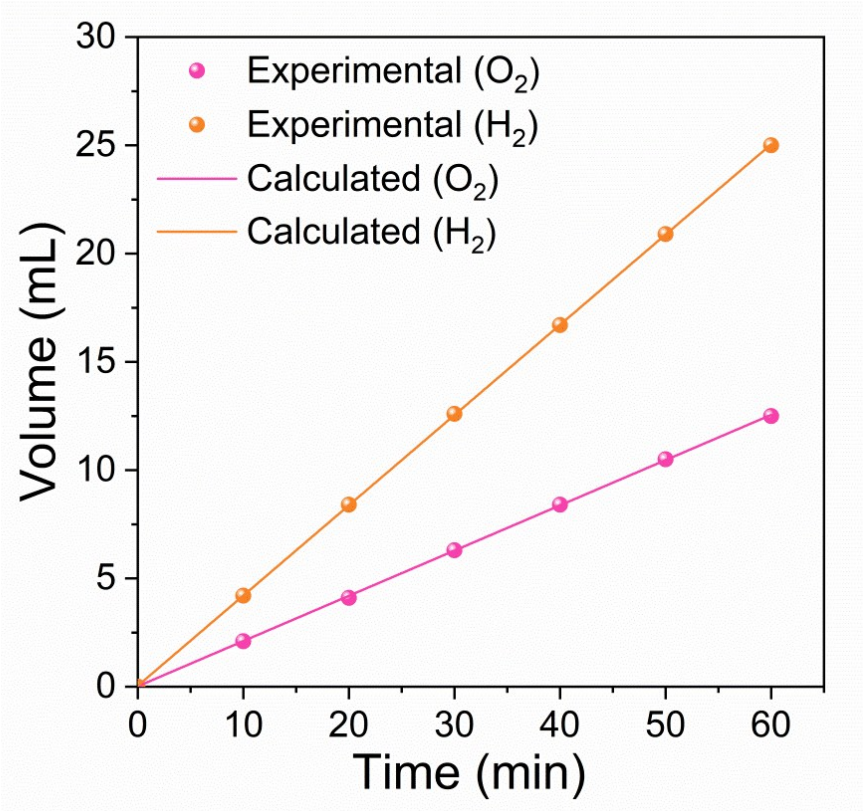


**Figure S18.** The experimental $H_2$ and $O_2$ production versus theoretical quantities for overall water splitting of $Ni_3S_2/VO_2$ at the constant current density.